Research Article

Surface and Adhesion Properties of a Softener Containing Fragrances Microencapsulated with Poly (Methyl Methacrylate) on Cotton, Polyester, and a Mixture of Cotton and Polyester Fabrics

Usaraphan Pithanthanakul and Vilai Rungsardthong*
Department of Agro-Industrial, Food and Environmental Technology, Faculty of Applied Science, Food and Agro-Industrial Research Center, King Mongkut's University of Technology North Bangkok, Bangkok, Thailand

Yulong Ding
Birmingham Centre for Energy Storage, School of Chemical Engineering, University of Birmingham, Birmingham, United Kingdom

* Corresponding author. E-mail: vilai.r@sci.kmutnb.ac.th DOI: 10.14416/j.asep.2023.05.001
Received: 9 February 2023; Revised: 11 March 2023; Accepted: 3 April 2023; Published online: 1 May 2023

Abstract
The distribution and adhesion of microcapsules on fabric surfaces are crucial factors for the production of long-lasting fragrance textiles. The objective of this research was to study the adhesion property of a softener containing microencapsulated fragrances on fabrics. Pink fruity fragrance (PF), and white floral fragrance (WF) were encapsulated with poly (methyl methacrylate) or PMMA, using the micro-suspension photopolymerization method, to form PF-PMMA, and WF-PMMA microcapsules, respectively. The particle sizes and zeta potential of the capsules were determined. The PF-PMMA and WF-PMMA were added to the fabric softener before being applied to three types of fabrics, cotton, TK (polyester), and TC (a mixture of cotton and TK). Surface morphologies of the fabrics treated with the softener were studied by scanning electron microscope (SEM). Interactions between the microcapsules and the fabrics were studied using a contract angle measurement device, Fourier Transform Infrared (FTIR) spectrometer, and Raman microscope. The average size of PF-PMMA was 484.8 ± 4.0 nm, smaller than that of WF-PMMA (664.6 ± 2.9 nm). Cotton was found to be hydrophilic with a rough surface due to cellulose fibers, while TK surface was smooth and hydrophobic. The different fiber structures and surface properties of the fabrics gave rise to different adhesion behavior, evidenced by the contract angle and Raman microscopic data. After 60 days of storage, the microencapsulated fragrances were found to remain on the cotton surfaces, but that on the TC and the TK surfaces disappeared. The results illustrated the interaction between the fabric surface and the microcapsules encapsulated with fragrances, which affected their adhesion. The knowledge obtained can be applied to the development of household products with long-lasting fragrances.

Keywords: Adhesion, Cotton, Fragrances-encapsulated, Polyester fabrics (TK), Poly (methyl methacrylate), TC fabrics

1 Introduction

Micro/nanoencapsulation is widely used in functional textiles for various functions, such as anti-bacterial [1], body temperature regulation [2], insect repelling [3], UV protection [4], and controlled release for long-lasting fragrances of the textiles [5]–[7]. The use of fragrances in consumer products not only delivers a pleasant sensory experience to the users but also enables the establishment of brand recognition for the products. The encapsulation of fragrances can prevent the evaporation of the volatile compounds in the fragrances and reduce degradation by the wall material [8]. The selection of the wall material and associated

preparation depends on the required characteristics of the microcapsules [9]. Besides, thermal and mechanical stabilities, particle size and distribution, and chemical reactivity of the microcapsules are all affected by both the wall and the core materials [10]. Synthetic polymeric wall materials used for textile applications include polyurethane, polyurethane, melamine-formaldehyde, polyamides, polyester, and poly (methyl methacrylate) or PMMA [5], [7]. Particularly, PMMA has received a lot of attention in recent years because of its ability to encapsulate volatile compounds [7], [11].

PMMA is a thermoplastic polymer commercially available and widely used for many years because of its safety, biocompatibility, low toxicity, and high chemical stability. PMMA has been used as a wall material for microencapsulation of various core materials, including cosmetic [12], pharmaceutical [13], thermal energy storage [14], [15], self-healing composites [16], [17], and textiles [7], [10], [18]. This polymer can be synthesized by the polymerization of methyl methacrylate (MMA) monomer with free radical and anionic initiations in the bulk, solutions, suspensions, and emulsions [19]. The most commonly used technique for PMMA microencapsulation is emulsion polymerization due to its simplicity to encapsulate hydrophobic materials [11]. PMMA nano/microcapsules have been treated on several fabrics, such as cotton, microfiber polyester fabrics, and cotton/polyester fabrics. The application of PMMA nano/microcapsules in fabrics was found to be highly durable and exhibited sufficient stability after multiple washing [11]. Photopolymerization provides an alternative route, which utilizes a light source that can be categorized by its wavelength, typically UV and visible light. Such a light source could also be provided by light-emitting diodes (LEDs), which have gained popularity as a visible irradiation source in recent years due to their environmental friendliness and potential to replace UV light sources [20], [21]. Light-activated polymerization offers a wide range of applications across multi-industrial sectors, including medicine, electronics, nanotechnology, and textile [22].

Fabric types and properties significantly influence the adhesion of the fragrances in the fabric softener to their surfaces. There are two types of fabrics: natural, and synthetic fabrics. Synthetic fibers occupy the main fiber manufacturing, accounting for approximately 64% of the global volume [23], expected to reach US$1.6 billion by 2026 (compound annual growth rate or CAGR of 3.2% from 2021 to 2026). In addition, the global market for cotton fiber is growing at a CAGR of 2.74% from 2020 to 2027. The blend of cotton and polyester fibers is a popular choice in the global market for fabric used in clothing. The global market of poly-cotton fabric may expand at 3% CAGR to $594.01 million by the end of 2033. These three types of fabrics are prevalent and present a high growth market trend. There are several reports on micro/nanoencapsulation for textile applications. He *et al.*, [24] investigated the retention and adhesion of melamine-formaldehyde (MF) microcapsules on a model fabric surface. The microcapsule retention and adherence on the model fabric surface were found to be improved by adding chitosan for the modification of cellulose. The adhesion mechanism between microcapsule and unmodified cellulose thin film was mainly due to the bridging force from the extension of cellulose molecule chains. Xiao *et al.*, [25] measured physicochemical properties and adsorption kinetics to explain the adsorption behavior and mechanism of double-encapsulated microcapsules (DEMs) onto cotton fabrics. The results illustrated the formation of intramolecular hydrogen bonds to facilitate a combination of DEMs and cotton fabrics. Pithanthnakul *et al.*, [7] prepared two types of microencapsulated fragrances (fruity and floral with PMMA by emulsion photopolymerization under blue-LEDs light and applied them to the softener for TC fabrics (a mixture of 20% cotton and 80% polyester) treatment. The remaining fragrances in TC fabrics, with microencapsulated fruity fragrances, and floral fragrances after 30 d storage, were as high as 54.3%, and 37%, respectively. The results showed the high potential to extend the fragrance release time by microencapsulating fragrances with PMMA using emulsion photopolymerization.

The distribution to surfaces and surface removal of microcapsules for textile application has attracted much attention in various fields, such as household care, drying, and cleaning [26]. Improving the adhesion and interfacial bond of microcapsules on each fabric is one of the crucial factors for textile applications to obtain long-lasting fragrances [10]. The fragrance-containing microcapsules are expected to be transferred to textile surfaces with good adhesiveness. However, particle filtration, fouling and cleaning led to particle removal from surfaces, which in turn would reduce

the adhesion [24]. Thus, a better understanding of the adhesiveness behavior between microencapsulated fragrances and textile surfaces is required. Therefore, this research aimed to investigate the adhesion of microencapsulated pink fruity fragrance (PF), and white floral fragrances (WF) with PMMA (PF-PMMA, and WF-PMMA) on three types of fabrics that present different properties of their surface, cotton, TK, and TC. The fragrances were microencapsulated without system deoxygenation since the oxygen removal process requires the use of expensive equipment. Thus, PMMA photopolymerization without system deoxygenation would lower the production cost for industrial applications. Surface morphology was studied by scanning electron microscope (SEM). Physical and chemical properties of the microcapsules and interaction between the microcapsules and fabrics, such as contract angle, Fourier transform infrared spectrometer (FTIR), and Raman microscope was determined.

2 Materials and Methods

2.1 *Materials*

Methyl methacrylate (MMA) containing ≤ 30 ppm hydroquinone monomethyl ether (MEHQ) as an inhibitor, was purchased from Sigma-Aldrich (MA, USA). Camphorquinone (CQ), ethyl 4-(dimethylamino) benzoate (EDMAB) as a co-initiator, and polyvinyl Alcohol (PVA) with a molecular weight of 30,000–70,000, 87–89% hydrolysate, employed as a polymeric surfactant was obtained from Sigma-Aldrich (MA, USA). Octadecane was supplied by Acros Organics (New Jersey, USA). The softener and two commercial fragrances: white floral fragrances (WF), and pink fruity fragrances (PF) were provided by Thai-China Flavours and Fragrances Industry Co., Ltd. (Nonthaburi, Thailand). The essential components of WF were phenylethyl alcohol, benzoyl acetate, and citronellol, which were combined to produce a delicate, flowery, and fresh rosy aroma. The primary components of PF were phenylethyl alcohol, terpineol, and geraniol, providing a gentle, sweet rose flowery aroma. Three bleached fabrics, cotton [100% cotton, No.32 (comb), extra combed S/J], TK [100% polyester, No.32 (ring), grade A], and TC [a mixture of 20% cotton and 80% polyester, No.30 (com), single] were bought from Sally-Textile Industry Co., Ltd. (Bangkok, Thailand). All other chemicals used were analytical grade.

2.2 *Methods*

2.2.1 Visible light photopolymerization of WF-PMMA and PF-PMMA

The fragrances, WF, and PF were encapsulated with PMMA microcapsules (WF-PMMA and PF-PMMA) by micro-suspension photopolymerization followed [7] with slight modification. Firstly, MMA monomers were mixed with each fragrance at a weight ratio that presented the highest conversion and encapsulation efficiency in our previous study [7], 3:1 and 1% of CQ and 0.6% of EDMAB (by weight) as co-initiators. The oil phase was formed by blending 2.5 g of MMA with co-initiators and mixing with a homogenous combination of each fragrance and 0.5 g of octadecane. The suspension was then poured into 45 g of 2% PVA (aqueous phase) and homogenized for 10 min with a high-speed homogenizer (T25 Digital, IKA, Germany) at a shear rate of 15,000 rpm. After stirring at 400 rpm for 50 min, MMA monomers were photopolymerized to PMMA for 6 h under a blue LED light without system deoxygenation before photopolymerization. The photoreactor comprised a blue-LED light and two plug light lamps with a wavelength range of 410–530 nm at an intensity of 10 W/cm^2. The system was covered with aluminium foil during the reaction, to avoid light exposure.

2.2.2 Fabric treatment

The fabric treatment was performed following Pithanthanakul [7] in our previous study. The fabric softener from a commercial formula consisting of water, softener base, Tween 20, and free PF or free WF at 93:5:1:1 (%w/w) was set as the control. The softener with the microencapsulated fragrances was prepared by mixing water, WF-PMMA or PF-PMMA microcapsules, and fabric softener base at 75:20:5 by weight. Each fabric, cotton, TK, and TC was cut into 5 × 5 in^2 and immersed into each mixture of the softener and distilled water (1:10 w/w) for 45 min. After drying at room temperature, all fabric samples were stored in an aluminum foil pouch (size 11 × 16 cm^2).

2.2.3 Particle size and zeta potential measurement

Particle size and zeta potential of the prepared PF-PMMA and WF-PMMA were analyzed using dynamic light scattering (DLS) at 658 nm, and laser doppler velocimetry (LDV) techniques using Malvern zeta sizer (Zeta sizer, Malvern Instruments, UK). The fresh emulsions were diluted by 100 times with deionized water and the stability of the microencapsulated fragrances was determined. Measurements were performed in triplicate at 25 °C after an equilibration time of 120 s.

2.2.4 Evaluation of fabric's surface hydrophobicity

The static contact angle of the droplet on the fabric surface was measured by a sessile drop method (KRÜSS model G10, Germany) to determine the wettability of the fabrics. Surface interaction between the surface of untreated fabric and softener containing microencapsulated fragrances droplets was measured by a 2-dimensional angle. The fabric with 3 × 3 cm^2 size was placed on a microscope glass slide on the stage for observation. After that, a 5 µL drop of liquid was applied on the fabric surface using a micro-syringe. The contact angle was measured after a single drop of the sample was dropped on the fabric surface. A camera and LabVIEW software were used for image capture and calculation by rotating the camera in a circle around the liquid drop at various angles and determining the average angle.

2.2.5 Characterization

2.2.5.1 Scanning electron microscopy

The morphological and elemental composition of the microcapsules on the treated fabric were analyzed by scanning electron microscopy, SEM (TM3030 Desktop SEM Microscope, Hitachi Ltd., Japan) equipped with a dispersive energy X-ray detector at an accelerating voltage of 15 kV. The fabric samples (cut into 0.3 × 0.3 cm^2) were coated with a thin layer (<20 nm) of sputtered gold using a sputter coater before the examination (Q150R ES, Quorum Ltd., Japan).

- Fourier transform infrared spectrometer

Each fabric treated with softener containing WF-PMMA, and PF-PMMA was prepared for the testing, with a size of 0.5 × 0.5 cm^2. FTIR spectroscopy was performed by an attenuated total reflectance Fourier transform infrared spectroscopy (Tensor 27 ATR-FTIR Spectrometer, Bruker Ltd., Germany) in the scanning range of 4000–400 cm^{-1}. Then, each fabric sample, and 1 mg of microencapsulated fragrance powders were placed on the sample beam of the spectrometer. The samples were placed on the diamond set, and their FTIR spectra were recorded and examined on a computer device and the data were normalized using OriginPro 9.0 (Originlab Co. Ltd., Northampton, USA).

- RAMAN

Raman analysis was performed on a Renishaw inVia Raman microscope system (Renishaw Plc., Wotton-under-Edge, UK). A 509/N.A. 0.75 objective and a 785-nm near-infrared (IR) diode laser excitation source (500mW, 5%) were used in all measurements. Spectra were recorded within the Raman shift window between 4000 and 100 cm^{-1} using a mounted charge-coupled device (CCD) camera with an integration time of 10 s in a single scan.

- Statistical analysis

One-way analysis of variance (ANOVA) with SPSS 11.6 for Windows was used to determine statistical significance (SPSS Inc., Chicago, III, USA). Duncan's multiple range test (DMRT) was performed to compare significant differences using a least-significant-difference ($p < 0.05$) mean.

3 Results and Discussion

3.1 *Particle size and zeta potential*

The DLS analysis presents the hydrodynamic diameter of nanoparticles dispersed within a suitable fluid. Table 1 demonstrated that the Z-average sizes of PF-PMMA and WF-PMMA were 484.8 ± 4.0 and 664.6 ± 2.9 nm, respectively. The Z-average sizes of PF-PMMA were smaller than the WF-PMMA, which was well corresponding to our previous study [6], [7]. The different galaxolide concentrations used as a fragrance fixative in WF and PF (17% and 1.4%, respectively) might lead to the different viscosity of each fragrance which affected the size of WF-PMMA microcapsules to be larger than PF-PMMA. The fixative exhibits a semi-solid property and highly viscous liquid at room temperature. However, both microcapsules present an average particle size as nanoscale. The intensity-

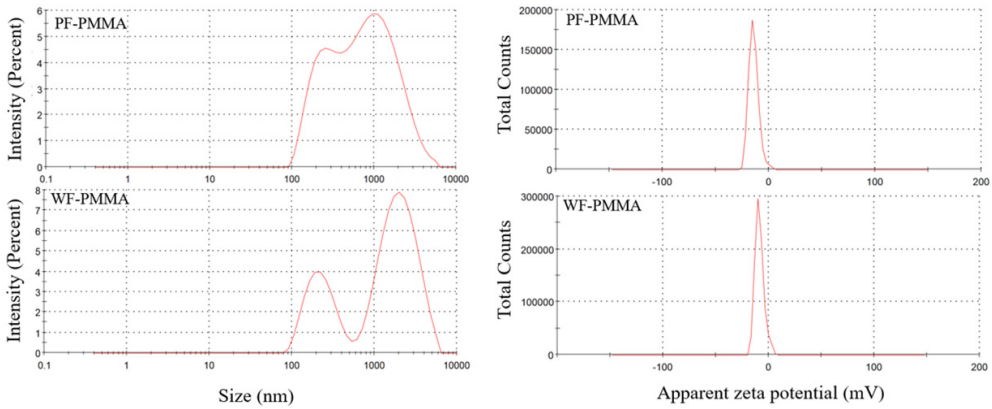

Figure 1: DLS size distribution intensity (A) and zeta potential distribution (B) of PF-PMMA and WF-PMMA.

particle size distribution of both samples was bimodal and separated into 2 peaks for WF-PMMA, as shown in Figure 1(a). The size distribution for PF-PMMA was average at 252.7 and 1273 nm for PF-PMMA while that of WF-PMMA was 234.8 and 2162 nm. A bimodal distribution might have resulted from the photopolymerization without system deoxygenation, then molecular oxygen inhibited free-radical polymerization, influencing the mechanical, and structural properties of the product obtained [27].

Table 1: Particle size, polydispersity index (PDI), and zeta potential of fragrances encapsulated with PMMA microcapsules

Samples	Z-Average Diameter (nm)	PDIns	Zeta Potential (mV)
PF-PMMA	484.8 ± 4.0^{a}	0.45	-14.3 ± 0.5^{b}
WF-PMMA	664.6 ± 2.9^{b}	0.59	-8.7 ± 0.3^{a}

Note: PF-PMMA and WF-PMMA mean pink fruity and white floral fragrances-encapsulated with poly (methyl methacrylate) microcapsules, respectively.

Different letters in the same column denote significant difference ($p < .05$).

SD: standard deviation from triplicate determinations

PF-PMMA and WF-PMMA had the PDI value of 0.45 and 0.59, and zeta potential at –14.3 ± 0.5 and –8.7 ± 0.3 mV, respectively, as represented in Table 1. The PDI measures the broad scope of molecular weight distribution. The wider the molecular weight, the higher the PDI. They are calculated by dividing the weighted average by the number of average molecular weights in the DLS system [28].

ISO standard publications 22,412:2017 describes that a PDI value that varies from 0.01 (mono dispersed particles) to 0.5–0.7 is classified as homogeneous, whereas the PDI value > 0.7 indicated the broad particle size distribution. Therefore, a PDI less than 0.7 indicated the good particle size distribution of PF-PMMA and WF-PMMA. Furthermore, another crucial parameter directly affects the emulsion stability is the zeta potential. Zeta potential greater than ±30 mV is generally considered to have a sufficient repulsive force that will decrease the droplet coalescence and achieve better colloidal stability [29]. However, the emulsions of PF-PMMA and WF-PMMA exhibited zeta potential of –8 to –15 mV, respectively, which were close to the threshold of agglomeration.

3.2 *Contact angle measurement*

The contact angle of the softener containing WF-PMMA, and PF-PMMA on the cotton, TK, and TC fabric surface, are presented in Figure 2(a)–(c). The surface wettability of various fabrics has a significant impact on polymer microcapsule adherence. The results show that the droplet of the softener containing WF-PMMA and PF-PMMA spread almost completely into cotton fabric within 3 min [Figure 2(a)] while more than 60% of the droplet still stayed on the surface of TC fabric even after 3 min passed [Figure 2(b)]. However, the droplet of both softeners permeated into the TK fabric as soon as it was dropped into the fabrics [Figure 2(c)]. Table 2 summarizes the contact angle of each experiment.

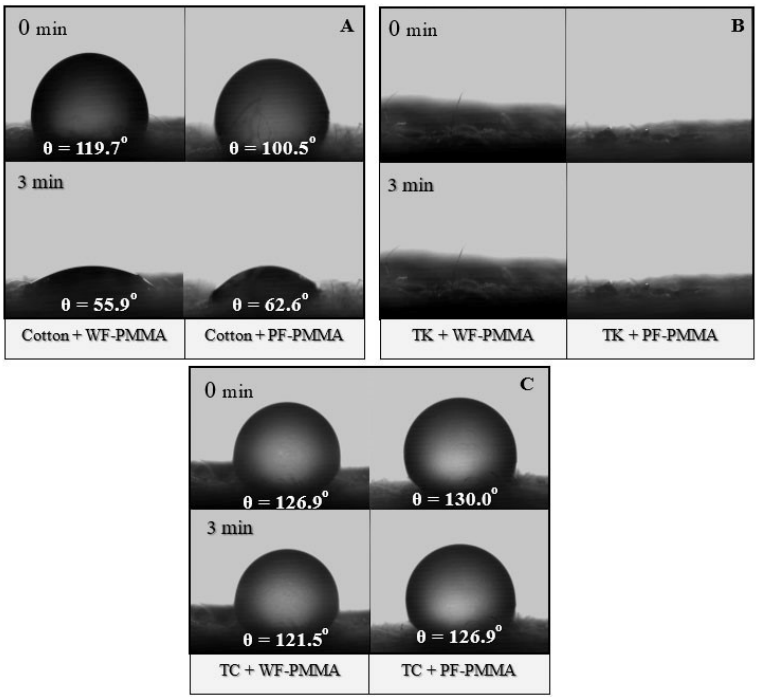

Figure 2: Contact angle of fabric softener containing WF-PMMA (left) and FP-PMMA (right) droplet on cotton (A), TK (B), and TC fabrics (C). Upper and lower row represent the different time (0 and 3 min) after dropping the same sample.

Table 2: Contact angle of fabric softener containing PF-PMMA, and WF-PMMA applied on three fabric types

Time (min)	Contact Angle (°)					
	Cotton		TK		TC	
	WF-PMMA	PF-PMMA	WF-PMMA	PF-PMMA	WF-PMMA	PF-PMMA
0	119.7 ± 0.7	100.5 ± 0.2	ND	ND	126.9 ± 0.3	130.0 ± 0.4
1	118.7 ± 0.2	86.7 ± 0.7			125.8 ± 0.3	128.6 ± 0.4
2	99.4 ± 1.0	75.1 ± 1.3			124.9 ± 0.4	127.5 ± 0.3
3	55.9 ± 4.9	62.6 ± 2.4			124.2 ± 0.4	126.9 ± 0.4
6	-	-			121.5 ± 0.5	103.1 ± 4.4
12	-	-			118.6 ± 0.6	61.9 ± 2.5
13	-	-			59.9 ± 1.6	-

Note: PF-PMMA and WF-PMMA mean pink fruity and white floral fragrances-encapsulated with PMMA microcapsules, respectively.
ND: Could not determined
SD: standard deviation from triplicate determinations

The contact angle of softeners containing WF-PMMA, and PF-PMMA in cotton fabrics rapidly shifted from 119.7° to 55.9° and 100.5° to 62.6° in 3 min, respectively. Meanwhile, both softeners were quickly absorbed into the polyester TK, and the contact angle could not be determined. However, TC fabric, which is made up of 20% cotton and 80% polyester, exhibited a contact angle that slightly shifted from 126.9° to 121.5° and from 130.0° to 126.9° in 3 min before reaching 59.9° and 61.9° after 13 and 12 min for softeners containing WF-PMMA, and PF-PMMA, respectively.

Contact angles of the softener with WF-PMMA are greater than those of softener containing PF-PMMA for a long time, which might be due to the higher hydroxyl groups (-OH) in PF [7]. As a result, the

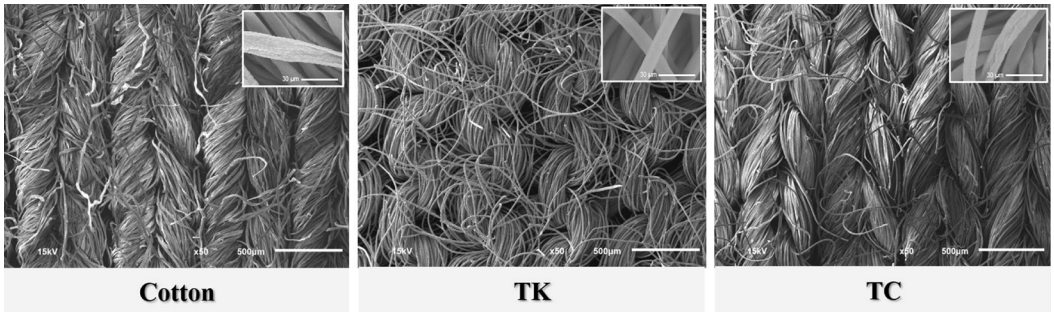

Figure 3: SEM images of untreated cotton, TK, and TC fabrics (500x). The insert shows the magnification with a scale bar of 30 μm (2000x).

softener with PF-PMMA could spread into the fabric faster. However, the contact angles of both softeners were >90° (high contact angle), which indicated unfavorable surface wetting. In general, there are more negative charges in polyester fabric than those in cotton fabric while PMMA also indicates negative charges. Hence, the contact angle of the softener containing WF-PMMA, and PF-PMMA droplets were greater than those on TC fabric. In general, there are more negative charges in polyester fabric than those in cotton fabric, while PMMA also indicates negative charges [30]–[32]. TK fabric is 100% polyester fiber, which has negative charges on its surface, while TC fabric, which composes of 80% polyester, tends to present negative charges too. The yarn spinning and weaving of each fabric also influence the fabric structure and compactness which influence the penetration and adhesion of the fabric softener. Consequently, the contact angle on TK fabrics could not be detected in this study. SEM images show the bundle of fibers in cotton and TC fabrics [Figures 3], which are high-bulk-filament yarn (bulky filament yarn). Compared to this, TK fabric [Figure 3] composes of short bundles of fibers that are twisted in one direction more loosely than bulky filament yarn, referred to as "spun yarn". Thus, softeners containing microencapsulated fragrances could easily penetrate the TK fabric. Consequently, fiber alignment is one of the factors affecting contact angle.

3.3 *Characterization of treated fabrics*

3.3.1 Scanning electron microscopy analysis

SEM insert images in Figures 3 reveal a clean surface morphology of the untreated cotton, TK, and TC fabric. Cotton fibers are composed of 90% cellulose and look like collapsed and twisted tubes, called "convolutions" [6]. TK fabric is a synthetic fiber containing oil/petroleum and has a relatively smooth surface morphology. TC fabric stands for "Tetoron cotton" where the polyester yarn makes up more than half of the total composition as reported in our previous work. Figure 4 shows the surface morphology of cotton, TK, and TC fabrics after treatment with a softener containing free fragrances versus microencapsulated fragrances. The surface morphology of the three types of fabric treated with softener containing free PF and untreated fabrics show no differences with, the fabric treated with free WF (image not shown). For all fabric types, the adhesion of WF-PMMA and PF-PMMA on the surface of fabrics changed the surface morphology of the fibers as observed in Figure 4. For the adhesion of the microencapsulated fragrances on the fabric surface, the results revealed that a layer of microencapsulated fragrances was distributed in the groove on the cotton fiber surface. This could be due to the lower contact angle of both microencapsulated fragrances on cotton fibers when compared to polyester fibers, implying that the adhesiveness was better for cotton fabrics. Furthermore, the SEM image shows more agglomeration of the larger WF-PMMA microcapsules on the fabric surface than the use of PF-PMMA, resulting from a greater viscosity of WF, which corresponds to our previous research [6], [7]. Figure 5 displays the surface element by a percentage of the treated fabric, determined by EDX analysis. The EDX spectra of cotton, TK, and TC fabrics after treatment with softener containing free PF, and each

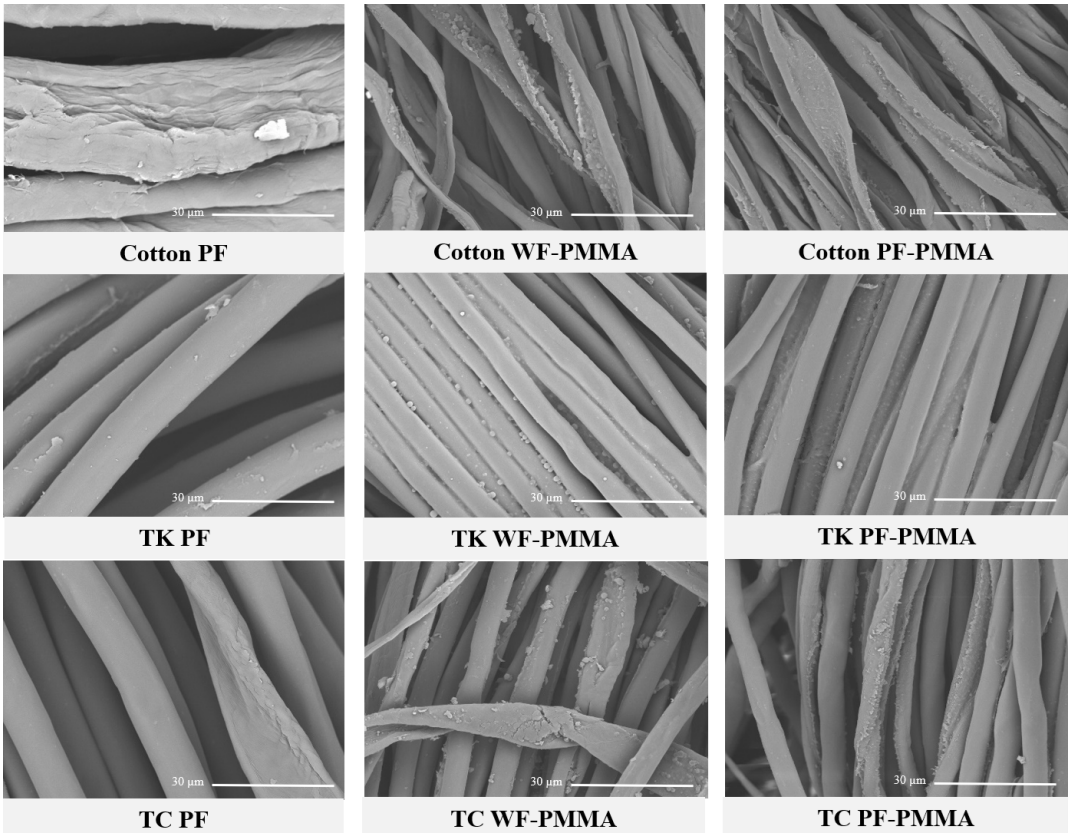

Figure 4: SEM image of cotton, TK, and TC fabrics treated with fabric softener containing the PF, WF-PMMA, and PF-PMMA (1000x).

microencapsulated fragrance were revealed. Figure 5 revealed that all fabrics treated with softener containing free PF showed only two peaks corresponding to carbon (C) and oxygen (O) elements, while the EDX spectrum of all fabrics treated softener with containing WF-PMMA, and PF-PMMA present the nitrogen (N) element in a range of 3.05–3.24%, indicating that the fiber surface is covered with microencapsulated fragrances. The N component in the fabric treated with encapsulated fragrances could come from the camphorquinone and ethyl-4-dimethylaminobenzoate (EDMAB) as the co-initiators were used in MMA polymerization to PMMA.

3.3.2 FTIR spectroscopy

FTIR spectra in Figure 6 show functional groups of both microencapsulated fragrances on the surface of three fabrics treated with softeners containing the microcapsules compared with commercial softeners (with free PF/WF). The IR spectra of WF-PMMA and PF-PMMA in Figure 6(a) reveal the absorption band of hydrogen bond O-H stretching vibration at 3438 cm^{-1}, and 3437 cm^{-1}, respectively, caused by the strong hydrogen bonds of WF and PF in microcapsules [7]. The peaks close to 2994 cm^{-1} and 2951 cm^{-1} are associated with C-H asymmetric and symmetric stretching, respectively. The sharp intense peak at 1739 cm^{-1} and the band at 1147 cm^{-1} represent C=O stretching of the ester group and -OCH_3 stretching vibration in PMMA, respectively.

The cotton fabric consists of cellulose and hemicellulose polymers [33]. The cotton, rich in functional groups of O–H, C-H, and C–O stretching vibrations were observed in the ranges of 3340–3290 cm^{-1}, 2900–2850 cm^{-1}, and 1054 cm^{-1}, respectively

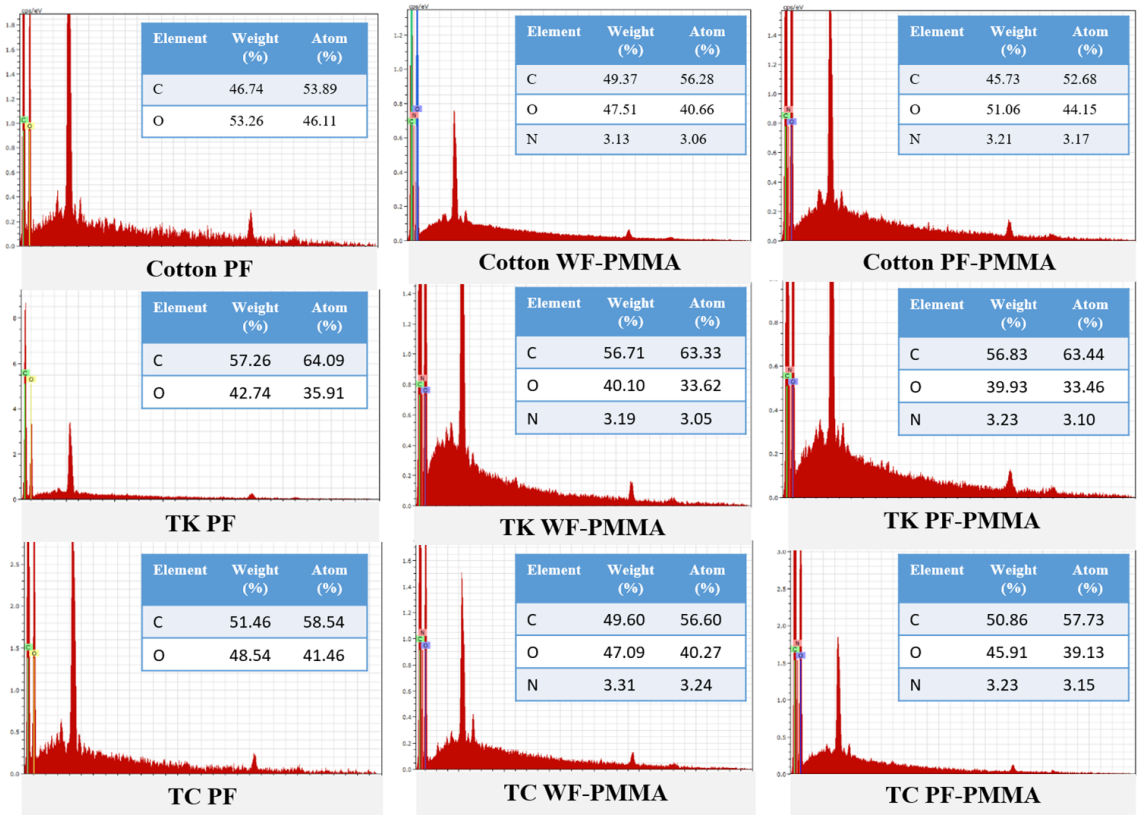

Figure 5: EDX spectra of cotton, TK, and TC fabrics treated with fabric softener containing the PF, WF-PMMA, and PF-PMMA.

[Figure 6(b)], which are all corresponding to the chemical structure of cellulose [34]. Besides, all bands in the range of 1500–800 cm^{-1} indicate the presence of C-H, O–H, C–O, and C–O–C bending vibrations, representing the cellulose. Compared with all treated cotton, IR spectra of cotton were detected in the cotton treated with any type of softeners. Nonetheless, it can be observed that the band at 2899 cm^{-1}, which is characteristic of the stretching vibration of C-H found in cellulose/hemicellulose was increased due to the strong C-H stretching in PMMA microcapsules, as shown in Figure 6(b).

In the case of TK, the peak of the hydroxyl group was absent in all samples of TK fabric. A weak band at 2967 cm^{-1} and 2914 cm^{-1}, attributed to the C-H stretch vibration was observed as shown in Figure 6(c). The high peak at 1713 cm^{-1} is assigned to C=O, which is an important characteristic of absorption in polyester. The characteristic spectra of C-O-C stretching vibration band at 1097 cm^{-1} and 1240 cm^{-1} were measured. The bands near 740 cm^{-1} represent the C=C stretching of the aromatic nucleus. All these peaks confirmed the existence of ester linkage. Figure 6(d) shows the IR spectra of TC fabric which shows the same pattern peak as observed in the IR spectra of TK fabric. Furthermore, the TC fabric showed an additional peak of the hydroxyl group (O-H) in the range of 3340–3290 cm^{-1} due to the composition of cellulose in cotton fibers. After treating TC fabric with softener containing WF-PMMA and PF-PMMA, the vibration band of C-H stretching showed slight shifting towards lower frequency at 2916 cm^{-1} and 2850 cm^{-1}, while the peak of the hydroxyl group was also increased. It can be confirmed that hydrogen bond is the main interaction that occurred between cotton fiber and both microencapsulated fragrances. This confirmed the adsorption of WF-PMMA and PF-PMMA onto the all-fabric surfaces.

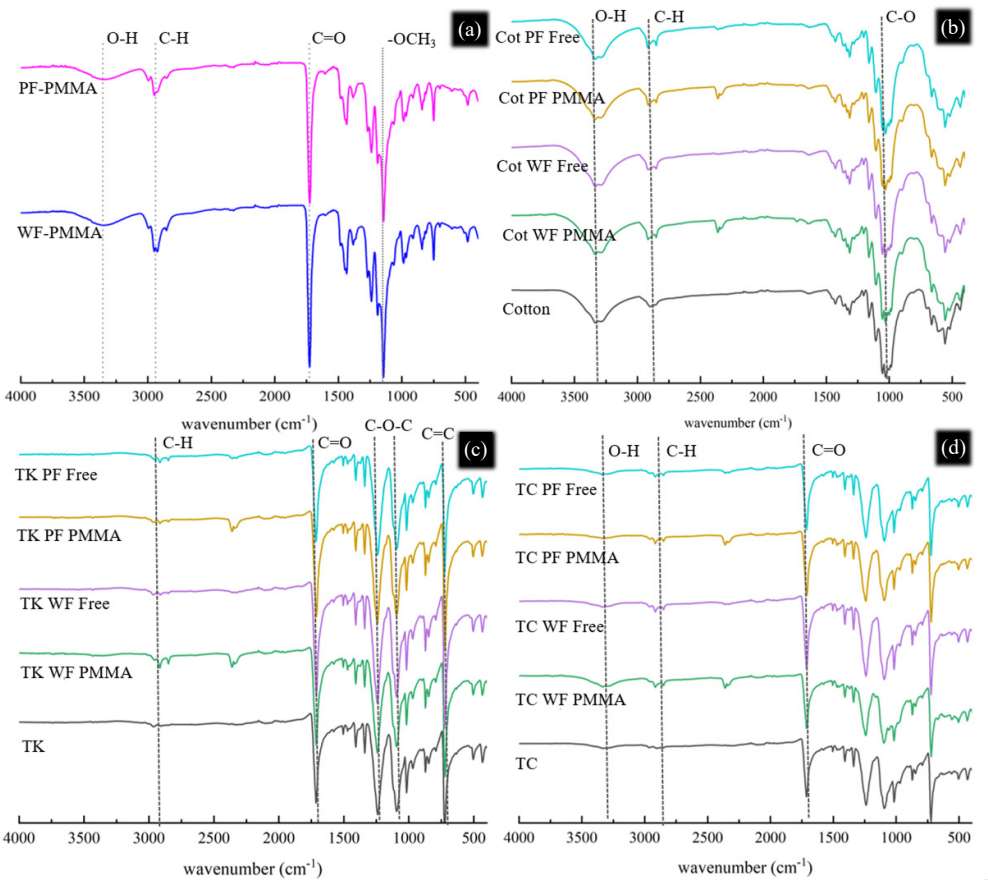

Figure 6: FTIR spectra of (a) the fragrances encapsulated microcapsules; and each fabric; (b) cotton, (c) TK, and (d) TC untreated, treated with free fragrances (WF and PF Free), WF-PMMA and PF-PMMA.

3.3.3 RAMAN

In addition to the FTIR results, Raman spectra (Figure 7) also confirmed the successful surface functionalization of untreated all types of fabrics treated with fabric softener containing free fragrance, and microencapsulated fragrances with PMMA. Raman spectra of the cotton and polyester fibers in TC fabric were used to represent fibers in cotton and polyester fabric since the samples were visualized at 100x magnification. In Figure 7, the Raman spectrum of cotton is not dominated by O-H bands as its infrared spectrum because O-H bonds are weakly polarizable in Raman, and water is usually "invisible" in Raman spectroscopy [35]. However, the cotton fibers showed that the Raman band was derived from cellulose, located at 2895 cm^{-1} (C-H stretching), 1475 cm^{-1} and 1380 cm^{-1} (CH_2 scissoring, and C-H bending), 1335 cm^{-1} (O-H bending), and 1122 cm^{-1} and 1094 cm^{-1} (C-O-C asymmetric and C-O-C symmetric stretching) [36], [37].

In the case of polyester fibers, the band at 1725 cm^{-1} represents the C=O stretching that can be observed at both IR and Raman, while the aromatic C=C stretching at 1614 cm^{-1} reveals the greater intensity in the Raman band [35], [38]. In comparison to untreated fabric or fabrics treated with fabric softener containing free fragrances, Raman spectra of cotton and polyester fibers treated with microencapsulated fragrances showed the presence of two prominent broad characteristic bands of C=O stretching and aromatic C=C stretching, which represent the strong interaction between the microencapsulated fragrances and fibers.

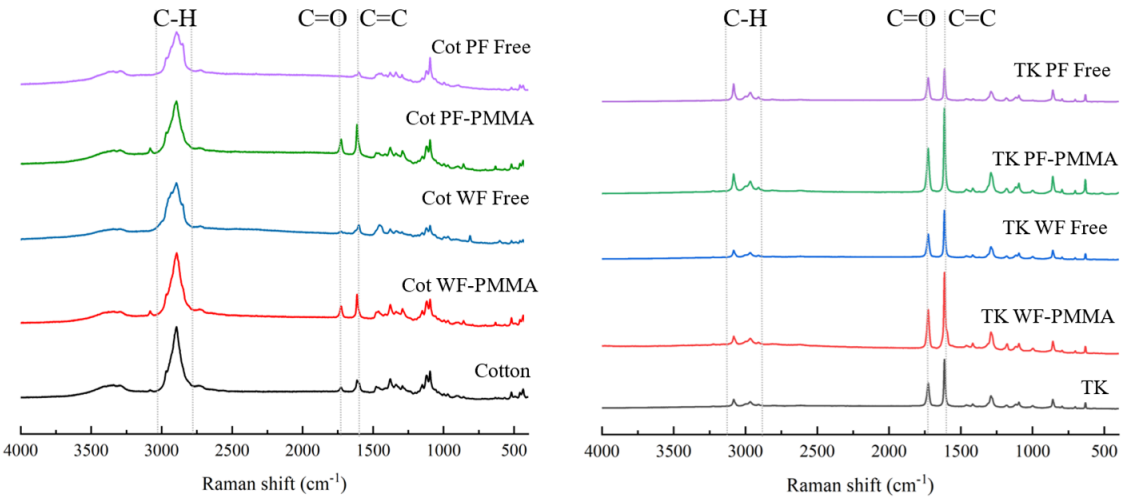

Figure 7: RAMAN spectrum of cotton fibers (Left) and polyester fibers (Right) untreated and treated with free fragrances (WF and PF Free), and fragrances encapsulated microcapsules (WF-PMMA and PF-PMMA).

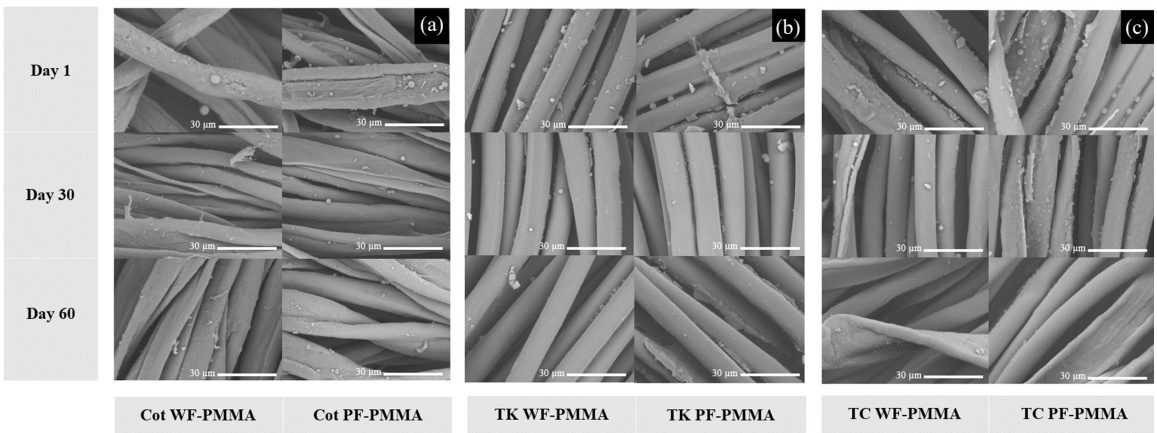

Figure 8: SEM image of (a) cotton, (b) TK, and (c) TC fabrics treated with WF-PMMA (left) and PF-PMMA (right) at 1, 30, and 60 days storage time.

3.4 *Durability of microencapsulated fragrances on treated fabrics*

Figure 8 shows SEM images of WF-PMMA and PF-PMMA adhesion on three types of fabrics after storage for 1, 30, and 60 days. The results were corresponding well with our previous study [6], [7] revealing that the microencapsulated fragrances relatively attached well to the surfaces of the cotton fabrics, especially in the groove of the cotton fibers. The adhesion might occur by the binding between the reactive groups of the microencapsulated fragrances with the hydrogen bonds on the cotton surface or by hydrophobic interaction with the polyester fibers. Some microcapsules that could not form the binding to the fabrics might be removed from the fibers after storage [25]. Furthermore, it could be observed that the larger microencapsulated fragrances (WF-PMMA) decreased and rarely appeared on TC, and TK fabrics after 60 days of storage. As a result of their larger surface area, the smaller PF-PMMA particles presented a better adhesiveness on the fiber surface, resulting in better storage stability [6], [39]. The results were corresponding with Monller [40] who studied the washout of

microcapsules on the fabric after the washing process. They reported that the larger microcapsules were washed out of the fibers in the first washing cycles and five washing cycles, which can be considered more or less constant until 20 washing cycles, and fabrics still smell peppermint after 20 washing cycles. The results indicated that the small microcapsules were still attached to the fabric. Several researchers reported that the principal factor that affects the adhesion of fragrance encapsulated in microcapsules on textiles is the particle size of the microcapsules.

The large surface energy and small-scale effect help the microcapsules to form a strong adhesion with fibers [25], [40]. Therefore, It could be confirmed in our previous research [6], [7] that the fabric treated with PF-encapsulated capsules showed the highest long-lasting fragrance even after 30 days of storage.

4 Conclusions

In this work, WF and PF encapsulated with PMMA capsules were prepared by photopolymerization without system deoxygenation, which resulted in a bimodal distribution of the microencapsulated fragrances. The TC fiber alignment and hydrophobic properties resulted in unfavorable surface wetting, which led to the highest contact angle of fabric softener containing WF-PMMA and PF-PMMA on TC fabrics. On the other hand, the lower contact angle of both microencapsulated fragrances (119.7° and 110.5°) on cotton fibers leads to better adhesion of the microcapsules on cotton fabric. The SEM and EDX images demonstrated the layer of the microcapsules distributed in the groove on the fiber surface. Furthermore, FTIR and Raman also confirmed the adsorption of WF-PMMA and PF-PMMA onto all fabric surfaces. After 60 days of storage, it was clear that the larger microcapsules mostly disappeared from all types of fabrics. The results revealed that the treated TC fabric with PF encapsulated capsule showed the highest long-lasting fragrance even after 30 days of storage as observed in our previous research [7]. It can be concluded that the smaller size of the microcapsules and hydrophilic properties of the fabric surface resulted in better adhesion of the encapsulated fragrances in PMMA microcapsules onto the fabric surfaces and revealed better storage stability. Understanding the adhesion behavior between microencapsulated fragrances and the fabric surfaces can facilitate the development of new formulations using microencapsulated fragrances in several household products.

Acknowledgments

Special thanks go to the Thailand Research Fund (TRF) under the Research and Researchers for Industries program (Contract No. PHD59I0013) and Thai-China Flavors and Fragrances Industry Co., Ltd. for their financial support.

Author Contributions

U.P.: investigation, methodology, formal analysis, writing– original draft; V.R.: funding acquisition, supervision, conceptualization, formal analysis, writing – review & editing; Y.D.: writing – review & editing.

Conflicts of Interest

The authors have declared no conflicts of interest for this article.

References

[1] S. Ghayempour and M. Montazer, "Micro/nanoencapsulation of essential oils and fragrances: Focus on perfumed, antimicrobial, mosquito-repellent and medical textiles," *Journal of Microencapsulation*, vol. 33, pp. 497–510, Aug. 2016.

[2] E. G. Saraç, E. Öner, and M. V. Kahraman, "Microencapsulated organic coconut oil as a natural phase change material for thermo-regulating cellulosic fabrics," *Cellulose*, vol. 26, pp. 8939–8950, Nov. 2019.

[3] S. Eyupoglu, D. Kut, A. O. Girisgin, C. Eyupoglu, M. Ozuicli, H. Dayioglu, M. Civan, and L. Aydin, "Investigation of the bee-repellent properties of cotton fabrics treated with microencapsulated essential oils," *Textile Research Journal*, vol. 89, pp. 1417–1435, Apr. 2019.

[4] D. Pargai and S. Jahan, "Application of vitis vinifera microcapsules on cotton fabric: A potential to prevent uv-induced skin problems," *Journal of Natural Fibers*, vol. 17, pp. 412–426, Mar. 2020.

[5] B. B. Podgornik, S. Šandrić, and M. Kert, "Microencapsulation for functional textile coatings with emphasis on biodegradability—A systematic review," *Coatings*, vol. 11, p. 1371, Nov. 2021.

[6] U. Pithanthanakul, S. Vatanyoopaisarn, B. Thumthanaruk, C. Puttanlek, D. Uttapap, B. Kiatthanakorn, and V. Rungsardthong, "Encapsulation of fragrances in zein nanoparticles and use as fabric softener for textile application," *Flavour and Fragrance Journal*, vol. 36, pp. 365–373, May 2021.

[7] U. Pithanthanakul, V. Rungsardthong, B. Kiatthanakorn, Chaiyasat, S. Vatanyoopaisarn, B. Thumthanaruk, D. Uttapap, and Y. Ding, "Visible light polymerization of poly (methyl methacrylate) to microencapsulate fragrances and application for fabric softener," *Industrial Crops and Products*, vol. 194, Jan. 2023, Art. no. 116329.

[8] D. R. Perinelli, G. F. Palmieri, M. Cespi, and G. Bonacucina, "Encapsulation of flavours and fragrances into polymeric capsules and cyclodextrins inclusion complexes: An update," *Molecules*, vol. 25, p. 5878, Dec. 2020.

[9] Y. Wang, H. Shi, T. D. Xia, T. Zhang, and H. X. Feng, "Fabrication and performances of microencapsulated paraffin composites with polymethylmethacrylate shell based on ultraviolet irradiation-initiated," *Materials Chemistry and Physics*, vol. 135, pp. 181–187, Jul. 2012.

[10] S. Alay Aksoy, C. Alkan, M. S. Tözüm, S. Demirbağ, R. A. Anayurt, and Y. Ulcay, "Preparation and textile application of poly (methyl methacrylate-co-methacrylic acid)/ n-octadecane and n-eicosane microcapsules," *The Journal of the Textile Institute*, vol. 108, pp. 30–41, Jan. 2017.

[11] F. Ahangaran, A. H. Navarchian, and F. Picchioni, "Material encapsulation in poly(methyl methacrylate) shell: A review," *Journal of Applied Polymer Science*, vol. 136, Nov. 2019, doi: 10.1002/app.48039.

[12] P. Teeka, A. Chaiyasat, and P. Chaiyasat, "Preparation of poly (methyl methacrylate) microcapsule with encapsulated jasmine oil," *Energy Procedia*, vol. 56, pp. 181–186, 2014.

[13] R. R. Mallepally, C. C. Parrish, M. A. M. Mc Hugh, and K. R. Ward, "Hydrogen peroxide filled poly(methyl methacrylate) microcapsules: Potential oxygen delivery materials," *International Journal of Pharmaceutics*, vol. 475, pp. 130–137, Nov. 2014.

[14] A. Sarı, C. Alkan, and A. Biçer, "Thermal energy storage characteristics of micro-nanoencapsulated heneicosane and octacosane with poly (methylmethacrylate) shell," *Microencapsulation*, vol. 33, pp. 221–228, Apr. 2016.

[15] S. Lashgari, A. R. Mahdavian, H. Arabi, V. Ambrogi, and V. Marturano, "Preparation of acrylic PCM microcapsules with dual responsivity to temperature and magnetic field changes," *European Polymer Journal*, vol. 101, pp. 18–28, Apr. 2018.

[16] Q. Li, A. K. Mishra, N. H. Kim, T. Kuila, K. Lau, and J. H. Lee, "Effects of processing conditions of poly(methylmethacrylate) encapsulated liquid curing agent on the properties of self-healing composites," *Composites Part B: Engineering*, vol. 49, pp. 6–15, Jun. 2013.

[17] F. Ahangaran, M. Hayaty, and A. H. Navarchian, "Morphological study of polymethyl methacrylate microcapsules filled with self-healing agents," *Applied Surface Science*, vol. 399, pp. 721–731, Mar. 2017

[18] K. Iqbal and D. Sun, "Synthesis of nanoencapsulated Glauber's salt using PMMA shell and its application on cotton for thermoregulating effect," *Cellulose*, vol. 25, pp. 2103–2113, Mar. 2018.

[19] D. Truffier-Boutry, X. A. Gallez, S. Demoustier-Champagne, J. Devaux, M. Mestdagh, B. Champagne, and G. Leloup, "Identification of free radicals trapped in solid methacrylated resins," *Journal of Polymer Science Part A: Polymer Chemistry*, vol. 41, pp. 1691–1699, Jun. 2003.

[20] Q. Cao, T. Heil, B. Kumru, M. Antonietti, and B. V. K. J. Schmidt, "Visible-light induced emulsion photopolymerization with carbon nitride as a stabilizer and photoinitiator," *Polymer Chemistry*, vol. 10, pp. 5315–5323, Sep. 2019.

[21] M. Abdallah, F. Dumur, B. Graff, A. Hijazi, and J. Lalevée, "High performance dyes based on triphenylamine, cinnamaldehyde and indane-1,3-dione derivatives for blue light induced polymerization A. for 3D printing and photocomposites," *Dyes and Pigments*, vol. 182, Nov. 2020, Art. no. 108580.

[22] Balcerak, J. Kabatc, Z. Czech, M. Nowak, and K. Mozelewska, "High-performance UV-Vis light induces radical photopolymerization using novel 2-Aminobenzothiazole-based photosensitizers," *Materials*, vol. 14, p. 7814, Dec. 2021.

[23] J. Egan and S. Salmon, "Strategies and progress in synthetic textile fiber biodegradability," *SN Applied Sciences*, vol. 4, Art. no. 22, Jan. 2022.

[24] Y. He, J. Bowen, J. W. Andrews, M. Liu, J. Smets, and Z. Zhang, "Adhesion of perfume-filled microcapsules to model fabric surfaces," *Microencapsulation*, vol. 31, pp. 430–439, Aug. 2014.

[25] Z. Xiao, W. Xu, J. Ma, Y. Zhao, Y. Niu, X. Kou, and Q. Ke, "Double-encapsulated microcapsules for the adsorption to cotton fabrics," *Coatings*, vol. 11, p. 426, Apr. 2021.

[26] Y. He, "Understanding the interactions between microcapsules and fabric surfaces," Ph.D. dissertation, School of Chemical Engineering, University of Birmingham, Birmingham, UK, 2013.

[27] M. Guvendiren, B. Purcell, and J. A. Burdick, "Photopolymerizable Systems," in *Polymer Science: A Comprehensive Reference.* Amsterdam, Netherlands: Elsevier, pp. 413–438, 2012.

[28] A. Shrivastava, "Polymerization," in *Introduction to Plastics Engineering*. Amsterdam, Netherlands: Elsevier, pp. 17–48, 2018.

[29] A. O. Elzoghby, M. S. Freag, and K. A. Elkhodairy, "Biopolymeric nanoparticles for targeted drug delivery to brain tumors," in *Nanotechnology-Based Targeted Drug Delivery Systems for Brain Tumors*. Amsterdam, Netherlands: Elsevier, pp. 169–190, 2018.

[30] R. Samu, A. Moulee, and V. G. Kumar, "Effect of charge and hydrophobicity on adsorption of modified starches on polyester," *Journal of Colloid and Interface Science*, vol. 220, pp. 260–268, Dec. 1999.

[31] H. Yang, K. Fang, X. Liu, F. An, "High-quality images inkjetted on different woven cotton fabrics cationized with P(St-BA-VBT) copolymer nanospheres," *ACS Applied Materials & Interfaces*, vol. 11, pp. 29218–29230, Aug. 2019.

[32] M. Wortmann, N. Frese, L. Hes, A. Gölzhäuser, E. Moritzer, and A. Ehrmann, "Improved abrasion resistance of textile fabrics due to polymer coatings," *Journal of Industrial Textiles*, vol. 49, pp 572–583, Nov. 2019.

[33] P. Prabhakar, R. K. Sen, M. Patel, Shruti, N. Dwivedi, S. Singh, P. Kumar, M. Chouhan, A. K. Yadav, D. P. Mondal, P. R. Solanki, A. K. Srivastava, and C. Dhand, "Development of copper impregnated bio-inspired hydrophobic antibacterial nanocoatings for textiles," *Colloids and Surfaces B: Biointerfaces*, vol. 220, Art. no. 112913, Dec. 2022.

[34] E. H. Portella, D. Romanzini, C. C. Angrizani, S. C. Amico, and A. J. Zattera, "Influence of stacking sequence on the mechanical and dynamic mechanical properties of cotton/glass fiber reinforced polyester composites," *Journal of Materials Research*, vol. 19, pp. 542–547, Apr. 2016.

[35] L. L. Cho, "Identification of textile fiber by Raman microspectroscopy," *Journal of Forensic Sciences*, vol. 6, pp. 55–62, Jan. 2007.

[36] V. K. Thakur, D. Vennerberg, S. A. Madbouly, and M. R. Kessler, "Bio-inspired green surface functionalization of PMMA for multifunctional capacitors," *RSC Advances*, vol. 4, p. 6677, 2014.

[37] S. Zhenyu, L. Zhanqiang, S. Hao, and Z. Xianzhi, "Prediction of contact angle for hydrophobic surface fabricated with micro-machining based on minimum Gibbs free energy," *Applied Surface Science*, vol. 364, pp. 597–603, Feb. 2016.

[38] K. J. Thomas, M. Sheeba, V. P. N. Nampoori, C. P. G. Vallabhan, and P. Radhakrishnan, "Raman spectra of polymethyl methacrylate optical fibres excited by a 532 nm diode pumped solid state laser," *Journal of Optics A: Pure and Applied Optics*, vol. 10, May 2008, Art. no. 055303.

[39] G. Nelson, "Microencapsulated colourants for technical textile application," in *Advances in the Dyeing and Finishing of Technical Textiles*. Amsterdam, Netherlands: Elsevier, pp. 78–104, 2013.

[40] P. Monllor, L. Capablanca, J. Gisbert, P. Díaz, I. Montava, and Á. Bonet, "Improvement of microcapsule adhesion to fabrics," *Textile Research Journal*, vol. 80, pp. 631–635, May, 2010.